ELSEVIER

Journal of Nuclear Materials 313–316 (2003) 116–126

journal of nuclear materials

www.elsevier.com/locate/jnucmat

Section 3. Plasma facing materials, coatings, and conditionings

New results from the tungsten programme at ASDEX Upgrade

R. Neu *, R. Dux, A. Geier, H. Greuner, K. Krieger, H. Maier, R. Pugno, V. Rohde, S.W. Yoon, ASDEX Upgrade Team

Max-Planck-Institut für Plasmaphysik, EURATOM-Association, Boltzmannstr.2, D-85748 Garching, Germany

Abstract

Since 1998 an increasing area of tungsten coated tiles has been installed at the central column of ASDEX Upgrade, reaching 7.1 m^2 in 2001/2002. The tiles were coated commercially by plasma arc deposition to a thickness of 1 μm. Post mortem analysis of the W-coating showed a strong erosion, which is attributed to ion sputtering, due to its two-dimensional variation. During the campaigns with W-coated central column, almost no negative influence on the plasma performance was found. Only during direct plasma wall contact or for reduced clearance in divertor discharges spectroscopic evidence for tungsten influx could be found. Effective sputtering yields of about 10^{-3} were derived, pointing to a strong contribution by light intrinsic impurities to the total W-sputtering. The increased W-content during plasma current ramp up decreases after X-point formation and the flux consumption during current ramp is only marginally enhanced compared to the graphite wall case. The W concentrations ranged from below 10^{-6} up to a few times 10^{-5}. In discharges with increased density peaking, a tendency for impurity accumulation was observed, which affected only a closely localized central region. Central heating led to a strong reduction of the central impurity content, consistent with neoclassical impurity transport.

PACS: 52.40.Hf

Keywords: Plasma–wall interactions; Tungsten components; High-*Z* material; Impurity transport; Erosion; First wall materials

1. Introduction

All major design studies of future fusion research and reactor devices employ tungsten as plasma facing component at least in the divertor region (see for example [1–4]) since in general, the erosion rate for low-*Z* materials like carbon or beryllium seems to be far too high in a steady state power producing device [1]. Additionally, the use of large area carbon based materials may lead to excessive codeposition of tritium causing a considerable safety problem [5].

On the other hand it became evident in recent years that in divertor devices with large areas of carbon based wall components the carbon impurity content is strongly influenced by the main chamber carbon source. This was observed spectroscopically in ASDEX Upgrade [6,7] as well as in JET [8] and recently in DIII-D [9]. During the successful W-divertor experiment in ASDEX Upgrade [10], no significant reduction of the carbon concentration was observed in the plasma bulk, despite the use of tungsten as plasma facing material (PFM) at the strikepoints. Moreover, strong carbon deposits on the inner strike point modules were found after the campaign [11], pointing to the fact that at least the inner divertor is a region were deposition dominates over erosion. Similar observations were made in JET using a Be-divertor, where C still was the dominant impurity [8].

Starting from these results and taking the constraints which will be imposed in a future tritium burning device into consideration, the logical step to take in ASDEX Upgrade was to investigate the role of an high-*Z* main chamber wall in a divertor tokamak. Here also the questions rise, to which degree it would be possible to

* Corresponding author. Tel.: +49-89 3299 1899; fax: +49-89 3299 1812.

E-mail address: rudolf.neu@ipp.mpg.de (R. Neu).

0022-3115/03/$ - see front matter
PII: S0022-3115(02)01386-7

reduce the C source in the main chamber, and while doing this, whether the plasma behaviour would change.

As will be described in the next section, the exchange of graphite tiles to W-coated tiles was done in a step by step approach to minimize the risk to experimental programme in the case of strong W contamination or failure of the coatings. Compared to the other divertor tokamak which uses high-Z (Mo) PFCs (Alcator C-Mod, see [12] and references therein), this has the advantage, that the stepwise approach may allow an easier identification of key elements in the plasma wall interaction. But it also bears the disadvantage, that the remaining carbon based PFCs may mask effects which will appear using metal walls alone. However, the strategy to counteract this will be outlined in the last section. This contribution will give an overview on the presently ongoing activities, which partly will also be published in more detail in accompanying papers [13–15].

2. The tungsten coating of the central column

The central column of ASDEX Upgrade was covered with tungsten coated graphite tiles in a step by step approach starting with experimental campaign 1999/2000 (PHASE I). There 1.2 m^2 of the lower part of the central column were coated by tungsten [16]. During PHASE II (campaign April 2001 to July 2001) a total tungsten coverage of the central column was applied, except for regions, which may be hit directly by the shine through of the neutral beam injection (NBI) or which are used as a limiter. Finally, the limiter region was also coated for the campaign 2001/2002 (PHASE III). In Fig. 1 the different positions of the W-tiles during PHASE I–III are indicated and an overview on the stages of the W programme in ASDEX Upgrade including the the W divertor experiment in 1996 is given in [17]. The increasingly larger surface area of tungsten coated tiles from campaign to campaign and the intention to use them at times as a limiter necessitated the identification of an industrial scale technique for coating several hundred tiles. The coating was chosen to be as thin as possible to keep mechanical stresses low, but also thick enough for the expected erosion and for a complete coverage of the substrate. For this purpose sample coatings on fine grain graphite obtained by magnetron sputtering and arc deposition were investigated. The main parameters for evaluating the coatings were their adhesion properties especially under thermal loading conditions, their content of light impurities, and the degree of surface coverage of these thin films on relatively rough fine grain graphite surfaces. The film thicknesses considered were in the range from 0.5 to 10 μm. Two types of graphite substrates were used (SGL Carbon R6710 and Schunk FU4206). The samples were pretreated mechanically to achieve an average surface

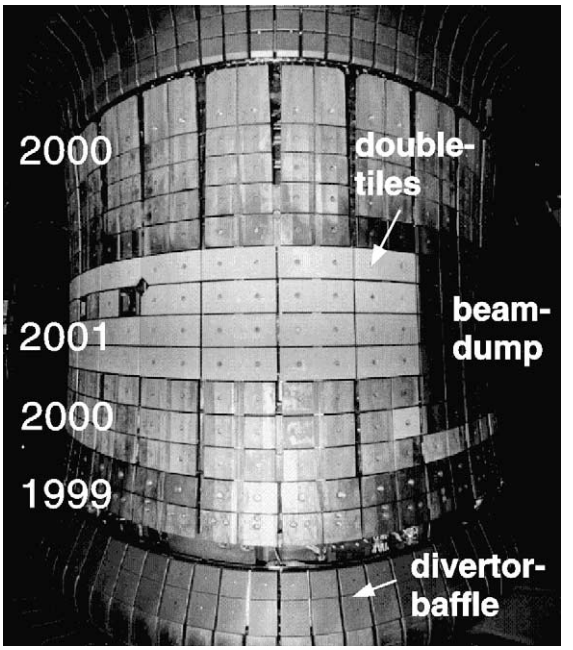

Fig. 1. The central column of ASDEX Upgrade with the tungsten coated tiles. The four rows in the equatorial plane are used as limiter during plasma start-up and in dedicated limiter discharges.

roughness of 1–1.5 μm for all substrates. Tungsten film thicknesses were determined gravimetrically in all cases and for some samples cross-calibrated by Rutherford backscattering spectroscopy. The surface coverage was excellent, even at film thicknesses below the average substrate roughness. The contents of light impurities measured by X-ray photo-electron spectroscopy in combination with sputter depth profiling was around 5–10 at.% for carbon and at or below the detection threshold of 1 at.% for oxygen. While the arc-deposited films showed no signs of delamination at any thickness and independent of the substrate material, it turned out to be impossible to deposit films with a thickness exceeding 3 μm by the sputtering method: Delamination occurred in form of small flakes with diameters up to the mm range. Thermal loading caused no failure up to the melting condition of the films, except for one case of a sputter deposited coating, which delaminated at a load of 11 MW/m^2. As a result of these investigation it was decided to choose 1 μm thick arc deposited W coatings from Plansee AG similar to the one shown in Fig. 2. More details about the procedures and results can be found in [18,19].

For the 2001 campaign (5.5 m^2 W-coating), the tiles were shaped similarly to those used during the 2000 campaign (see for example [16]). In the present campaign (2001/2002) also most of the start-up limiter region (equatorial ring at the central column) is tungsten coated

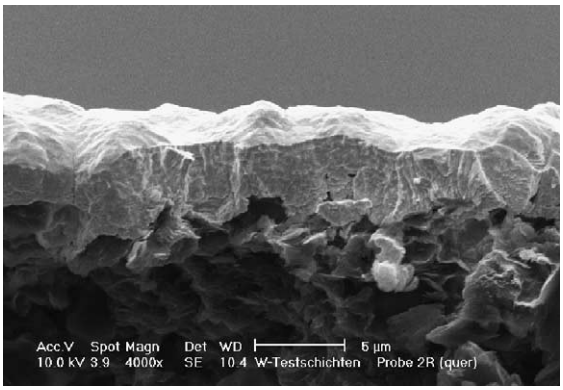

Fig. 2. SEM cross-sectional imaging of a 4 μm thick plasma-arc W coating similar to the type used during PHASE II and PHASE III.

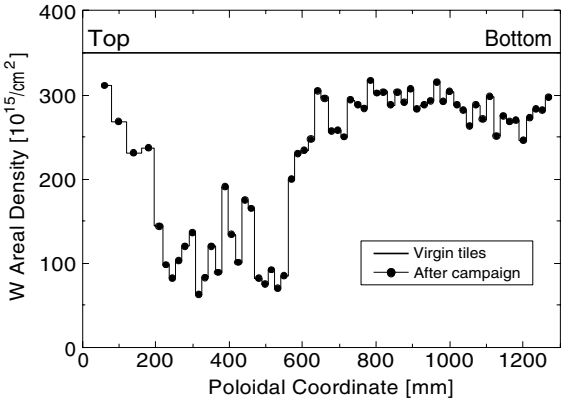

Fig. 3. Erosion pattern of W-coated test tiles mounted during PHASE II. The poloidal coordinate denotes the distance along the tile surfaces from the top edge of the heat shield.

with so called 'double-tiles' (see Fig. 1). These tiles diminish the number of leading edges and due an improved mount the evolution of misalignment is reduced. Recent thermal screening tests for these complete tiles indicated also the possibility to use them at the position of the NBI dumps, the only position where still uncoated CFC tiles are in use. During these tests the coated tiles were subject to power loads above 30 MW/m^2 during 0.3 s from the ion beam test facility MARION of the FZ Jülich. No macroscopic damage of the coatings was observed, only after inspection with a SEM microcracks in the order of 100 nm became evident. However, due to their very small extension and since no signs of exfoliation were visible, it was decided that their use in ASDEX Upgrade is feasible. In parallel to these tests with graphite substrates, two-dimensional (Dunlop DMS 704) and three-dimensional (SEP N11) CFC substrates were coated with similar tungsten films, to serve as an alternative solution at the beam dumps and other regions with high power loads. Again the surface coverage is excellent in spite of the even rougher surface structure of CFC as compared to fine grain graphite. Concerning the stress state of the films X-ray diffraction measurements were performed [19]. As in the case of graphite substrate all observed stresses were compressive. For the 2D material Dunlop DMS 704, there is a distinct variation of the stress depending on the direction parallel or perpendicular to the fibre planes. In the case of the 3D material a rather homogeneous stress is observed which is much lower than in the case of the ordinary graphite substrate. The consequences of these stress states to the behaviour under thermal loading will be investigated in the future.

3. W erosion and migration

During PHASE II, a complete column of W-coated test tiles with a W-layer thickness of 60 nm was installed to allow a sensitive measurement of a poloidal erosion profile. The tiles were measured ex-situ by ion beam analysis using RBS and sputter Auger electron spectroscopy (AES) [20]. The analysis revealed a maximum of the poloidal W-erosion profile above the midplane (see Fig. 3). The measured erosion exceeded the one expected from sputtering by charge exchange particles alone by at least one order of magnitude. Considering also the observed toroidal variation, it became evident that the predominant erosion channel was due to ion impact. Indeed, spectroscopic measurements of the W influx during plasma operation in PHASE III, as well as recent Langmuir probe measurements at the central column, point to the fact, that the erosion flux is dominated by the current ramp up and ramp down phase, when the central column is used as a limiter. Due to the trapezoidal cross-section of the tiles, there are also areas, which are shadowed from the incident field lines. There, an AES analysis revealed a deposited layer consisting mainly of carbon, oxygen and silicon with a thickness of 20–30 nm on top of the tungsten coating [21]. Details on the post mortem analyses of tiles will be presented in [13].

Beside the erosion through plasma particles, arc tracks have been found on the tiles at the lower end of the central column after PHASE I [21] and on marker probes. The number of observed tracks depends on the position of the tile and especially at the position of the baffle of the inner divertor a large number of tracks was visible. They eroded the whole layer thickness in a region about 100 μm broad and several mm long. From the neighbouring graphite region it seems that there occur less arcs. Whether this is only due to their reduced visibility on the graphite or whether the W surface is more prone to arcs will be a matter of future investigations. The migration of tungsten was investigated by the measurement of the deposition on graphite and CFC

tiles [20,13]: Only about 10% of the eroded material is found in the divertor. These may be attributed to the fact that the main erosion is during the limited phase of the discharges, where no parallel transport to the divertor is possible. Additionally, the analyses of graphite tiles in the main chamber reveal that W is very locally redeposited, with an effective poloidal e-folding length of 2.5 cm [13].

In order to understand the W transport mechanisms in the SOL, calculations with the DIVIMP 2D Monte-Carlo impurity transport code [22] have been started [14]. DIVIMP treats trace impurities on a background plasma, which at ASDEX Upgrade is usually taken from B2/EIRENE [23] calculations. Since in DIVIMP the area of plasma ion–wall interaction is restricted to the divertor where the flux surfaces intersect the wall, it had to be extended to accommodate for the tungsten source at the central column. Therefore a simple model was implemented where the plasma parameters were extrapolated from the outermost grid ring to the appropriate points of the wall assuming an exponential decay of the electron density as well as the electron and ion temperatures. First calculations show that the results sensitively depend on this decay length and that the qualitative features of the erosion and deposition measurements can be reproduced [14].

4. Investigations on W spectroscopy

During the W-divertor campaign a technique was developed to derive the W concentrations from spectroscopic signatures in the vacuum UV (VUV) around 5 nm [24]. These investigations were complicated by the rather complex structure of the spectra exhibiting a so called quasicontinuum structure originating from $\Delta n = 0$ transitions in tungsten ions around W^{29+}. The spectra of the individual ionisation states become simpler by going to shorter wavelengths and therefore to $\Delta n = 1$ transitions. Spectra taken in the spectral range from 5.5 to 8 Å and 15–19 Å for plasmas with central temperatures up to 5 keV revealed a large number of lines, originating from $3l$ to $4l'$ transitions (M-shell $\Delta n = 1$ transitions) of ionisation states from W^{39+} to Cr-like W^{50+} [25]. The identification is performed by comparison with ab initio structure calculations and the intensities were derived from a collisional radiative model [26,27] and from ion densities calculated with the impurity transport code STRAHL ([28] and references therein).

In Fig. 4 a measured spectrum after W-injection is compared to a simulated one. At the central temperature of 5 keV the spectrum is dominated by spectral lines from Zn-like to Co-like W and hints for contributions of Fe- to Cr-like W can be found. For the simulation a uniform W-concentration (c_W) of 5×10^{-5} was adopted,

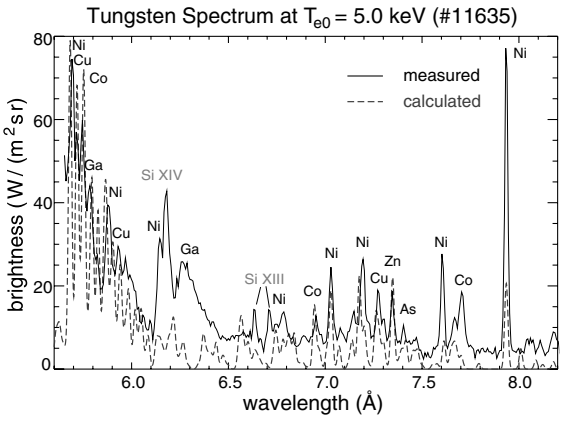

Fig. 4. X-ray spectrum of tungsten together with the theoretical predictions, in the range from 5.5 to 8.2 Å measured with a KAP crystal (discharge #11635, $T_{e0} \approx 5.0$ keV during W-injection). The spectral lines arising from intrinsic Si are marked.

which may not be the case over the complete radius, i.e. for the whole range of ionization states. Nevertheless the agreement with the experiment is quite satisfactory.

For the routine monitoring of the central W content, the spectral line at 7.94 Å originating from W^{46+} was chosen. The Ni-like W^{46+} ion exists over the large temperature range from 2.5 to 5 keV, enabling a sensitive detection of W. The line is measured with a temporal resolution of 10 ms by a high resolution Johann spectrometer which has a high throughput and allows the clear distinction from other intrinsic impurities (as Fe or Cu), exhibiting lines in the same spectral region.

Together with the measurement of the W-quasicontinuum, this yields a sensitive measurement of the central c_W for the usual range of central T_e in ASDEX Upgrade (1–5 keV). For $T_e > 2.5$ keV it even allows the extraction of some profile information of the W-concentration.

For the measurement of the W influx two arrays of 10 fibre guides each were installed, allowing the independent monitoring of every single row of W-tiles. The influx was determined from the brightness of the WI line at 400.8 nm using the inverse photon efficiency ($S/XB \approx 10$) which may vary by a factor of 2 depending on the actual edge temperature [29].

5. Operation with W start-up limiter and large area W walls

The experimental campaign of PHASE II was started without additional wall conditioning by boronization or siliconization to run the plasma discharges with the pure tungsten surface. During this initial period the total radiation and the Z_{eff} were higher than for a well conditioned machine, but this was attributed to the high

oxygen content (few percent). A dedicated program to investigate the performance of tungsten as PFM was executed and all relevant scenarios were tested. After two weeks of operation, a boronization was applied to reduce the oxygen content of the discharges. Since it became evident from the post mortem analyses of the test tiles in PHASE II, that there are strongly erosion dominated areas throughout the whole central column (see Section 3), it was decided to omit this initial phase, and to start with boronization already from the beginning of PHASE III. A significant amount of tungsten influx was only measured during plasma start-up and in specially designed discharges, which had low clearance with respect to the tungsten tiles (or when using the tungsten tiles as limiter.) A 5 MW additionally heated H-mode plasma had been radially shifted towards the central column from the nominal clearing of 12 cm down to 4 cm. The W-influx rose from a value below the detection limit to $\approx 2.5 \times 10^{18}$ m^{-2} s^{-1}. Calculating the D-flux to the wall by using the brightness of the simultaneously measured D_δ and $S/XB = 6000$ an effective sputtering yield $Y_{\mathrm{eff}} \approx 0.8 \times 10^{-3}$ is derived. Obviously, this cannot be due to pure D sputtering since this would require ion temperatures in the range of 100 eV. But taking sputtering by light impurity ions (O, C) into account, temperatures in the range of 10–20 eV, as measured by a Langmuir probe, are sufficient [11,30] to yield a consistent result. Together with assumptions on the active surface and from the increase of the W-content, a penetration probability for tungsten released from the central column in the order of 1% could be derived [31]. However, it should be kept in mind that the erosion pattern observed by the post mortem analyses is very inhomogeneous making the above extracted value rather uncertain.

The H-mode regime comprises by far the largest operational space in ASDEX Upgrade, and therefore, most of the experimental data are gathered in the H-mode at low ($\delta \approx 0.15$) to intermediate ($\delta \leqslant 0.45$) triangularities. For low δ, tungsten concentrations around 10^{-6} or below were observed. Quite a lot of information can be extracted already from the so called 'standard H-mode' discharge (see Fig. 5) which is run almost every day of operation [32]. It is designed to check the heating and the diagnostic systems and to document the conditioning of the device. After the measurement of the L–H threshold (power ramp by chopping one NBI source) a first phase at natural H-mode density with a second power ramp (performed by ICRH) to $P_{\mathrm{aux}}^{\mathrm{heat}} \approx 5$ MW follows. In the second part a density plateau at 80% of the Greenwald density limit ($\bar{n}_{\mathrm{e}} = 10^{20}$ m^{-3}) is run. During the initial phase with one NBI source only, the particle confinement is rather high, as indicated by the strong increase of the natural density. Adding the ICRH power the natural density is quickly reduced and it slightly increases when switching from ICRH to the

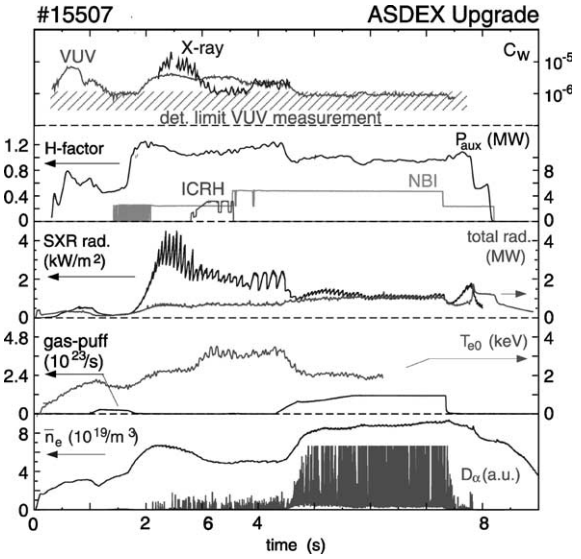

Fig. 5. Temporal behaviour of a 'standard' H-mode discharge in ASDEX Upgrade ($I_{\mathrm{p}} = 1$ MA, $B_{\mathrm{t}} = -2.0$, $q_{95} = 3.2$ and $\delta = 0.15$). The H-factor is calculated according to the ITER98P ELMy H-mode scaling.

second beam source. Throughout the discharge the main chamber radiation is very low. This general behaviour is reflected in the W-concentration, which reaches its highest value just at the beginning of the H-mode phase. By comparison of the concentration extracted from the VUV measurement (W-quasicontinuum, stemming from regions with $T_{\mathrm{e}} \approx 1$ keV) with the one extracted from the W^{46+} (central emission) a peaking of the W-concentration profile at $t = 2.5$ s becomes evident. This peaking is inverted during the ICRH phase and after switching to NBI only, the c_{W}-profile flattens at a value of (2–3) $\times 10^{-6}$. During the high density phase no W-signal is detected in the SXR. This is due to the fact that the temperature is too low for the existence of W^{46+} and to a further decrease of the W-concentration as it is deduced from the measurements in the VUV. The value of $c_{\mathrm{W}} = 10^{-6}$ (from the VUV measurement) during the high density phase has to be seen as an upper limit, since the complexity of the quasicontinuum radiation makes the distinction from the background radiation very difficult. During the start-up phase of the discharge ($t = 0.5$–0.8 s) with a direct plasma contact to the tungsten surface, an increased W-concentration is observed, which decays quickly after the evolution of the X-point in the plasma. A similar process can be observed during current ramp-down (from $t = 7.8$ s) as the increase of total radiation indicates. Measurements of the W-quasicontinuum in other discharges show that the tungsten concentration there reaches values even around 10^{-4}. This is due to the fact that the auxiliary heating ($P_{\mathrm{NBI}} = 2.5$ MW) leads to higher W-sputtering than

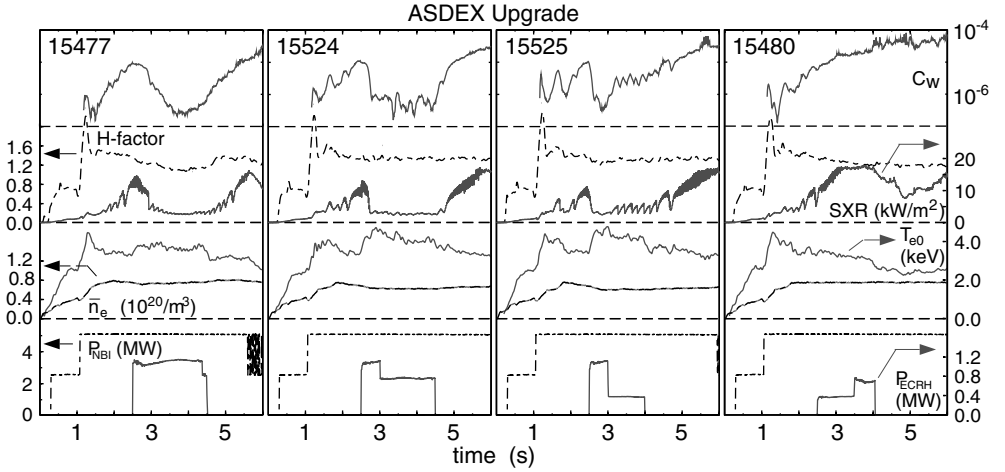

Fig. 6. Behaviour of similar improved H-mode discharges $I_p = 1$ MA, $B_t = -2.5$ T, $\delta = 0.35$, showing enhanced c_W with NBI only (first row: c_W; second row: H-factor, SXR-radiation; third row: line averaged density $\bar{n}_e$, central temperature T_{e0}; fourth row: additional heating power NBI (P_{NBI}), ECRH (P_{ECRH})). The W content could be controlled by the amount of additional central ECRH.

during the ohmic current ramp-up, consistent with the Langmuir probe measurements.

In discharges with $\delta \approx 0.4$ the tungsten concentrations were higher by about a factor of 5, reflecting the generally better particle confinement also seen for the natural density at a given current and heating power. Performing this kind of discharges with moderate constant gas-puffing at intermediate heating powers from NBI ($P_{NBI} \leqslant 7.5$ MW) yields a very high energy and particle confinement at densities around or above the Greenwald limit. The reason for this seems to be a reduction of the energy/particle transport in cases where the heating is applied further off axis, as proposed by Stober et al. [33]. A further ingredient of these discharges is the slowly evolving density peaking of the background ions which could be explained by a very small inward velocity of the order of the neoclassical Ware-pinch [33]. Density peaking accompanied by a weak temperature gradient is the natural prerequisite for neoclassical impurity accumulation, which amplifies the density peaking proportional to the charge of the impurities [34], as will be discussed below in more details. Therefore these discharges were prone to higher central c_W reaching values above 10^{-5}, which increases during the whole discharge [31].

Advanced scenarios are the second important experimental topic at ASDEX Upgrade. Especially improved H-modes are given some emphasis since they can be performed in quasi steady-state [35]. They are characterized by fishbones instead of sawtooth activity and show no central barrier but generally improved confinement over ordinary H-modes. An enlargement of the operational space for the improved H-mode towards higher densities was gained by running the discharges at $\delta \approx 0.35$ [36]. As in the ordinary H-modes at medium triangularity, the tungsten concentration showed a slow increase to values above $c_W \approx 10^{-5}$ throughout the whole duration of the discharge (see Fig. 6), which again was accompanied by an increasing density peaking.

In parallel to the improved H-mode discharges, other routes to advanced tokamak operation were pursued, namely high-β discharges as well as discharges with electron ITBs. In both cases the highest performances were obtained during PHASE II and III [36]. From the viewpoint of the tungsten contamination, they were completely unaffected and c_W stayed mostly below the detection limit of the VUV as well as the SXR diagnostics.

Limiter discharges play a very minor role in the experimental program of ASDEX Upgrade. Common to these discharges is the impact of high energy ions to the tungsten surfaces, which results in increased W-erosion and W-influx. Due to direct contact of W-flux to the last closed flux surface its penetration to the confined region is also more likely. Conventional L-modes had been only of operational interest during PHASE II, in order to explore their behaviour in regard to the plasma start-up at a fully tungsten covered central heat shield foreseen for PHASE III. Several discharges at intermediate densities, ohmic as well as with additional heating powers up to 5 MW were performed during PHASE II. During these discharges the plasma was shifted radially and vertically towards the tungsten tiles. As expected, the W-concentration increased during the plasma contact with W surfaces to values around 10^{-5}. However no serious accumulation was observed for the discharge parameters considered.

Limiter discharges were also used to keep an L-mode edge in discharges with additional heating powers, which lie considerably above the L–H transition threshold for

divertor operation, in order to explore ITB discharges. In such discharges the central tungsten concentration rose quickly after switching on the neutral beams and the formation of the barrier. This scenario resulted in the highest tungsten concentrations and values above 3×10^{-4} were measured, leading to an eventual radiation collapse of the barrier. After the loss of the ITB the central tungsten concentration generally dropped and the onset of sawteeth resulted in a further reduction of c_W. Consequently, as in an ordinary limiter discharge, the plasma often completely recovered from the former high W-inventories and reached tolerable tungsten concentrations. This kind of discharges was only seen as an interim solution for better suited divertor discharges finally performed in PHASE III. There, the ion ITBs were run with an early transition to the divertor and showed a much lower W-concentrations (more than a factor of 10) as their limiter pendant. Due to the short duration of all the ITB discharges it is not clear whether they already reached their steady state impurity content.

During PHASE III, special emphasis has been given to the analysis of the start-up phase at the tungsten start-up limiter. As deduced from the limiter experiments in PHASE II a higher W-contamination during start-up (and ramp-down) was expected. This led to the questions whether this higher W-content would deteriorate the build-up of the plasma current and whether the initially high W concentration would decay strongly enough when switching to divertor operation. Hints that the impurity contamination would decrease rapidly enough are seen in the experiments with siliconization in ASDEX Upgrade [37] and the operation of Alcator C-Mod [12]. However, both cases are slightly different since tungsten as a high Z-material could behave differently to Si and the operation of Alcator C-Mod is at higher densities and higher specific ohmic power. A detailed investigation of several parameters during start-up at the graphite surface and the tungsten surface for different stages of surface conditioning revealed, that the increase of the flux consumption with W-limiter is below 5% compared to values from the boronized graphite limiter. From the erosion measurements cited above, it can also be excluded that deposited layers (boron from boronization, carbon from deposition) mask the effect of W, because parts of the W area were found to be strongly erosion dominated. The plasma current ramp is not hampered in any way as might be also concluded from radiation measurements, which were highest with siliconized graphite walls. The boronizations led to a strong reduction of the radiation independent of the material of the tiles. Going from PHASE II to PHASE III an increase in c_W by about a factor of 2, especially during the early start-up phase is observed, but the effect of the boronizations is even larger where a reduction of c_W by up to a factor 5 is observed. The W concentration increases within about hundred discharges to its initial value showing that the boron layer is quickly eroded again. For more details on these investigations, the reader should refer to [17]. The behaviour of the carbon content was deduced from the CVI Lyman-α brightness I_{CVI} in 'standard H-mode' discharges and is presented in [31,17]. A long term decrease in the CVI brightness is visible, especially since the regular application of the siliconization. Although no siliconization was applied during PHASE II and PHASE III and large areas of new graphite surfaces were introduced before PHASE II (installation of the new divertor IIb, see [38]) I_{CVI} is at the lower end of the observed range. This points to a carbon reduction by a factor of 1.5–2 due to the W-coatings.

There was no strong impact of the tungsten coated wall on the general plasma behaviour, except for the ITB discharges with L-mode edge described above. The only obvious difference to previous campaigns was the significant reduction of the H-mode threshold by 20% measured also in the 'standard' H-mode discharge [32,38]. At the moment it is not clear whether this reduction is related to the tungsten coated heat shield or to changes in the edge plasma due to the modified divertor. According to the experiences after long term vents the W-coating obviously facilitates a faster conditioning of the machine.

6. Peculiarities of W-transport

The central tungsten concentration depends strongly on impurity transport, as already indicated in the previous section. The impurity transport is governed by the continuity equation. Under steady state conditions this leads in the source free region to

$$\frac{1}{n_I^{eq}} \frac{dn_I^{eq}}{dr} = \frac{d \ln n_I^{eq}}{dr} = \frac{v}{D}. \tag{1}$$

The diffusion coefficient consists of an anomalous and a neo-classical part $D = D_{an} + D_{neo}$. The convective contribution, which is a prerequisite for impurity accumulation is normally assumed to be purely neo-classical with $v = v_{neo}$. Considering only collisions of impurity and main ions, one gets for the normalized impurity density gradient

$$\frac{d \ln n_I^{eq}}{dr} = \frac{d \ln n_D}{dr} \frac{Z_I}{Z_D} \frac{D_{neo}}{D_{neo} + D_{an}} (1 - H\eta_D), \tag{2}$$

where Z_I, Z_D are the charges of the impurity ions and the background ions and $H \approx 0.2$–0.5 represents the so called impurity screening, which depends on the collisional regime. $\eta_D = (d \ln n_D/dr)/(d \ln T_D/dr)$ is the ratio of the normalized temperature gradient to the normalized density gradient of the background ions. From this equations one can easily see that a necessary

ingredient for impurity accumulation is a density gradient (density peaking) of the main ions. This gradient is amplified by Z_I/Z_D, which is typically 40–50 for W in ASDEX Upgrade plasmas and will be ≈70 in a burning plasma. It is diminished through the anomalous diffusion and the term in parentheses. This term appears critical because it may vary from small positive numbers to small negative numbers: typically the normalized temperature gradient is significantly larger than the density gradient in the confinement region and hence the product $H\eta_D$ is in the order of one.

Accumulation becomes evident not only from the W-concentration measurements but also from the radiation profile. Fig. 7 shows the behaviour of the plasma radiation for an ensemble of plasma discharges with low to high auxiliary heating power (P_{aux} = 3–14 MW). They are selected because of their complete diagnostic coverage and comprise all discharge scenarios run at ASDEX

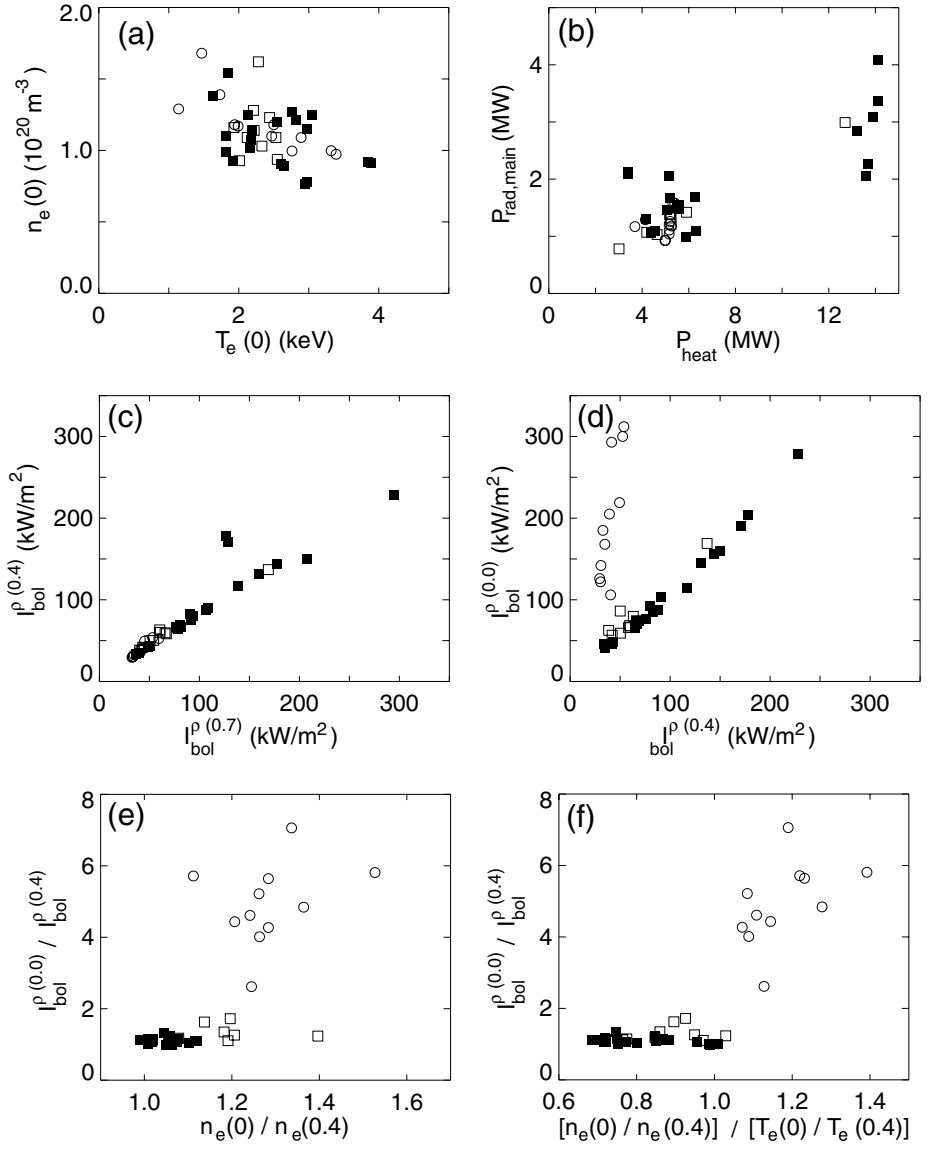

Fig. 7. Comparison of discharges with and without central impurity accumulation (filled symbols: discharges with central wave heating. Circles: discharges without sawteeth or fishbones). (a) Central electron densities $n_e(0)$ versus central temperatures $T_e(0)$. (b) Total main chamber radiation $P_{rad,main}$ versus total heating power P_{heat}. (c) Comparison of line integrated radiations measurements for a peripheral bolometer channel $I_{bol}^{\rho(0.7)}$ with $\rho_{tangential}^{pol} = 0.7$ and one at intermediate tangential radius $I_{bol}^{\rho(0.4)}$. (d) See (c), showing the brightness for a central channel $I_{bol}^{\rho(0.0)}$ versus $I_{bol}^{\rho(0.4)}$. (e) Central radiation peaking $I_{bol}^{\rho(0.0)}/I_{bol}^{\rho(0.4)}$ versus central density peaking $n_e(0.0)/n_e(0.4)$. (f) Central radiation peaking versus $[n_e(0.0)/n_e(0.4)]/[T_e(0.0)/T_e(0.4)] \approx \eta_D^{centr}$.

Upgrade with sufficiently long steady state conditions (medium triangularity with phases of constant gas puff, ELM-free, ELM type I and II, advanced H-modes, high β_N). The ratio of the number of data points with and without central radiation peaking is not representative. Accumulation appears only under the circumstances cited below, which exist in a very minor part of all discharges. The dataset comprises discharges with a factor four variation in central temperatures and a factor of 2 in central densities. The total main chamber radiation is low and usually amounts to 25–40% of the heating power. For the typical temporal evolution of most of these discharge scenarios the reader should refer to [31]. The features of the dataset are the following:

- In discharges without accumulation the radiation is strongly dominated by edge radiation because the line integrated radiation is almost equal for the bolometer channels with different tangential radii $\rho_{tang} = 0, 0.4, 0.7$.
- In phases with accumulation the enhanced radiation is only visible on central channels ($\rho_{tang} < 0.2$). No increase of the total radiation is observed.
- Only discharges with very long ELM free periods show increased radiation at intermediate radii.
- Central wave heating (ICRH or ECRH) prevents from centrally peaked radiation profiles.
- Density peaking alone is not sufficient for accumulation, but the ratio of the normalized gradients η_D in Eq. (2) is an important ordering parameter. In our investigation this critical parameter is linked to the loss or the absence of sawteeth or fishbones.

Typical conditions for such centrally peaked radiation profiles are low to intermediate heating power without central wave heating, where the anomalous diffusion is low. In these cases, the central radiation is increased by all impurity species existent in the plasma as seen by spectroscopic measurements. The very small affected volume explains that for similar influxes, strongly different (>factor of 10) central impurity contents may be observed. Finally, this effectively overrides any correlation between influx and impurity content in discharges with accumulation. In the discharges chosen for the above data-set mostly a combination of NBI and a minor part ICRH is used to stabilize neoclassical tearing modes (NTMs) by reducing the density peaking [39]. This is obviously completely sufficient to prevent also from impurity accumulation. Hints for such a beneficial behaviour during ICRH have also been found in tungsten test limiter experiments in TEXTOR [40]. As a side remark it should be mentioned that (3/2) NTMs do not lead to reduction of impurity peaking, since they cause confinement degradation which is obviously located at larger radii. The above considerations clearly point to the tool which may be used to quench accumulation: An increase of D_{an} at the critical position decreases ($d \ln n_D/dr$), ($D_{neo}/(D_{neo} + D_{an})$) and increases $H\eta_D$. Since the affected volume is very small, the central accumulation can be suppressed very efficiently by central heating *without* strongly degrading the total confinement.

A dedicated power scan for the 'impurity pump-out' effect was performed in improved H-mode discharges ($I_p = 1$ MA, $B_t = -2.5$ T, $P_{NBI} = 5$ MW, $\delta = 0.35$). These discharges show very good confinement ($H_{ITER-H98y} \approx 1.3$) at intermediate densities with peaked density profiles and a continously rising W-concentration [31]. In a series of discharges the central ECRH-power was varied from zero (reference discharge) up to 1.2 MW (3 gyrotrons) as shown in Fig. 6. For the highest ECRH power applied (1.2 MW) a very strong reduction of c_W by more than a factor of 30 and the onset of sawteeth is observed, but at the same time the energy confinement is also degraded. Using 0.4 MW of ECRH, the confinement is not affected, but also the c_W is not decreased. The most successful results where achieved when starting with 3 gyrotrons and reducing the power after 0.5 s. In these cases, both effects, the reduction of c_W and the good confinement are maintained. In all cases the discharges return to their initial behaviour after switching off ECRH. The process may be explained within the framework developed above: coupled to the low energy transport in these discharges the anomalous particle transport is also decreased, allowing that even a very small drift velocity leads to a density peaking [33]. This density peaking together with low anomalous transport and a moderate peaking of the temperature profiles provokes the neoclassical impurity accumulation. The central wave heating obviously counteracts this in several ways. Due to the stiff temperature profiles the central thermal transport is increased and the observed coupling to the particle transport [33] causes flatter density profiles of the background ions which lead to the reduction of the neoclassical inward drift. Together with the increased anomalous transport this finally yields a strong reduction of the central impurity content. A quantitative description of the impurity transport calculations for the above discharges is given in [15]. There it could be shown that the peaking of the total radiation as well as of the W-concentration almost entirely can be explained by neoclassical impurity transport.

7. Conclusion and outlook

Since 1998 an increasing area of tungsten coated tiles has been installed at the central column of ASDEX Upgrade, reaching an area of 7.1 m^2 in 2001/2002 representing about 85% of the total area of the central column. The W-coating is applied by plasma arc depo-

sition to a thickness of 1 μm, and the coated tiles have proven to fulfil all the requirements of ASDEX Upgrade, even when used at the position of the beam dumps. The post mortem analyses of the W-coating show erosion yields which are larger by at least one order of magnitude compared to the value expected for sputtering by charge exchange particles. The two-dimensional variation of the erosion proves that this erosion is due to ions, which at least partly is attributed to the plasma start-up and ramp-down. Measurements of the migration show that W is mostly redeposited very locally. Beside the erosion through plasma particles, arc tracks have been found on the tiles at the lower end of the central column and on marker probes. Spectroscopic measurements in the VUV and in the SXR spectral region provide a sensitive measurement of the central W-concentration and allow the extraction of profile information of c_W. No negative influence on the plasma performance was found, except for ITB limiter discharges. The flux consumption for current ramp at a tungsten surface is only 5% larger as in the graphite wall case. Only during direct plasma wall contact or for reduced clearance in divertor discharges spectroscopic evidence for W-influx was found. From these observations effective sputtering yields of about 10^{-3} could be derived, pointing to a strong contribution by light intrinsic impurities. The tungsten concentrations ranged from below 10^{-6} up to a few times 10^{-5}. The increased W-content during plasma current ramp-up rapidly decreases after X-point formation. In discharges with increased density peaking, a tendency for increased central tungsten concentrations or even accumulation was observed. The region affected is very closely localized within $\rho_{pol} \leqslant 0.2$. Central heating led to a strong reduction of the central impurity content, which can be described quantitatively by neoclassical impurity transport simulations. Simultaneously, only a very benign reduction of the energy confinement is observed.

A further reduction of carbon is necessary in order to access a regime where the plasma edge is not dominated by low-Z radiation. On the road to this goal additional parts, originally made of graphite will be coated. For autumn 2002 the installation of W-coated tiles for the beam dumps, the upper passive stabilizer loop and the baffle region at the inner divertor are foreseen. In the course of these reconstructions, all the tiles of the central column will be exchanged to ones of the new design (double tiles), all of them freshly coated with W. As a consequence about 15 m^2 of PCFs will be covered by a virgin W surface, only the divertor regions and the guard limiters on the low field side will still consist of graphite based components. This will provide an answer the initial question whether the migrating carbon had an influence on the results so far. Depending on the results on the ongoing thermal screening tests, even the coating of the guard limiters is envisaged.

Extrapolation of the ASDEX Upgrade results to ITER or other devices is difficult, as long as (edge) transport is not fully understood. Although edge modelling is in progress [14,41] further benchmarking is necessary, to obtain at least for the single case of ASDEX Upgrade consistent results. These will strongly depend on the knowledge of the background plasma edge which still evolves. It has to be kept in mind that this is also true for carbon based materials (see for example C-migration and flake production), although there is already a long lasting experience in a large number of devices. Since the behaviour of W is found to be consistent with neoclassical transport, no W accumulation is expected for the ITER standard scenario, according to earlier investigations [42]. The recipe to prevent central accumulation by central heating may be fulfilled in a natural way by central alpha particle heating, although the power density will be lower in ITER. Additionally, peaking of the background density caused by the neoclassical ware pinch will play only a very minor role. However, in scenarios with otherwise peaked density profiles, a prediction of the accumulation behaviour is uncertain due to the unknown ratio of the gradients and the level of anomalous transport. Concerning the start-up limiter, tungsten may be an alternative to the currently planned Be-limiter in ITER when following the very benign behaviour observed in ASDEX Upgrade, under the assumption of a similar edge plasma in ITER.

References

[1] G. Janeschitz, ITER JCT, ITER HTs, J. Nucl. Mater. 290–293 (2001) 1.
[2] D. Meade et al., in: Proceedings of the 18th IAEA Conf. on Fusion Energy, Sorrento, Italy, 2000, (CD-ROM), IAEA, Vienna, 2000, pp. IAEA-CN-77/FTP2/16.
[3] F. Najmabadi, S. Jardin, M. Tillack, L. Waganer, ARIES Team, in: Proceedings 18th IAEA Conference on Fusion Energy, Sorrento, Italy, October 2000, (CD-ROM), IAEA, Vienna, 2000, pp. IAEA-CN-77/FTP2/15.
[4] S. Nishio et al., in: Proceedings of the 18th IAEA Fusion Energy Conference, Sorrento, Italy, vol. FTP2/14, 2000.
[5] G. Federici et al., J. Nucl. Mater. 266–269 (1999) 14.
[6] A. Kallenbach, R. Neu, W. Poschenrieder, ASDEX Upgrade Team, Nucl. Fusion 34 (1994) 1557.
[7] R. Pugno et al., J. Nucl. Mater. 290–293 (2001) 308.
[8] G. McCracken et al., Nucl. Fusion 39 (1999) 41.
[9] D. Whyte et al., Nucl. Fusion 41 (2001) 1243.
[10] R. Neu et al., Plasma Phys. Control. Fusion 38 (1996) A165.
[11] K. Krieger, H. Maier, R. Neu, ASDEX Upgrade Team, J. Nucl. Mater. 266–269 (1999) 207.
[12] B. Lipschultz et al., Nucl. Fusion 41 (2001) 585.
[13] K. Krieger et al., in: Proceedings of the 15th International Conference on Plasma Surface Interaction, Gifu, Japan, 2002. PII: S0022-3115(02)01351-X.

[14] A. Geier et al., J. Nucl. Mater., in press. PII: S0022-3115(02) 01519-2.
[15] R. Dux, C. Giraud, R. Neu, K. Zastrow, J. Nucl. Mater., in press. PII: S0022-3115(02)01508-8.
[16] R. Neu et al., J. Nucl. Mater. 290–293 (2001) 206.
[17] R. Neu et al., Fusion Eng. Des., in press.
[18] H. Maier et al., Surf. Coat. Technol. 142–144 (2001) 733.
[19] H. Maier et al., in: Proceedings of the 10th International Conference on Fusion Reactor Materials, Baden-Baden, Germany, 2001.
[20] K. Krieger, V. Rohde, J. Roth, W. Schneider, ASDEX Upgrade team, in: Proceedings of the 10th International Conference on Fusion Reactor Materials, Baden-Baden, Germany, 2001, Europhysics Conference Abstracts.
[21] W. Schneider et al., in: Proceedings of the 28th EPS Conference on Controlled Fusion and Plasma Physics, Funchal, 2001, Europhysics Conference Abstracts.
[22] P. Stangeby, J. Elder, J. Nucl. Mater. 196–198 (1992) 258.
[23] R. Schneider et al., J. Nucl. Mater. 196–198 (1992) 810.
[24] K. Asmussen et al., Nucl. Fusion 38 (1998) 967.
[25] R. Neu, K.B. Fournier, D. Bolshukhin, R. Dux, Physica Scripta T 92 (2001) 307.
[26] K. Fournier, At. Data Nucl. Data Tables 68 (1998) 1.
[27] K. Fournier, APS 2001 and private communication (2001).
[28] R. Dux et al., Nucl. Fusion 39 (1999) 1509.
[29] A. Thoma et al., Plasma Phys. Control. Fusion 39 (1997) 1487.
[30] V. Philipps et al., Plasma Phys. Control. Fusion 42 (2000) B293.
[31] R. Neu et al., Plasma Phys. Control. Fusion 44 (2002) 811.
[32] F. Ryter et al., Plasma Phys. Control. Fusion 44 (2002) A407.
[33] J. Stober et al., Nucl. Fusion 41 (2001) 1535.
[34] G. Fussmann et al., Plasma Phys. Control. Fusion 33 (1991) 1677.
[35] O. Gruber et al., Phys. Rev. Lett. 83 (1999) 1787.
[36] A. Sips et al., Plasma Phys. Control. Fusion 44 (2002) A151.
[37] V. Rohde et al., in: Proceedings of the 18th IAEA Conference, Fusion Energy, Sorrento, Italy, October 2000, (CD-Rom), pp. IAEA-CN-77/EXP4/24, IAEA, Vienna, 2001.
[38] R. Neu et al., Plasma Phys. Control. Fusion 44 (2002) 1021.
[39] J. Stober et al., Plasma Phys. Control. Fusion 43 (2001) A39.
[40] G. Van Oost et al., in: Proceedings of the 22th EPS Conference on Controlled Fusion and Plasma Physics, Bournemouth, 1995, Europhysics Conference Abstracts, vol. 19C, part II, EPS, Geneva, 1995, p. 345.
[41] G. Federici et al., Review talk on PSI Gifu, J. Nucl. Mater., in press. PII: S0022-3115(02)01327-2.
[42] R. Dux, A.G. Peeters, Nucl. Fusion 40 (2000) 1721.